AGU PUBLICATIONS

Geophysical Research Letters

RESEARCH LETTER
10.1002/2016GL071885

Key Points:
- Site amplification term is different between surface waves and vertically-incident shear waves
- Amplification maps for Southern California, based on 1-D profiles, can be very different
- Waveforms from the El Mayor Cucapah earthquake support a different site term definition between wave types

Supporting Information:
- Supporting Information S1

Correspondence to:
D. C. Bowden,
dbowden@caltech.edu

Citation:
Bowden, D. C., and V. C. Tsai (2017), Earthquake ground motion amplification for surface waves, *Geophys. Res. Lett.*, *44*, 121–127, doi:10.1002/2016GL071885.

Received 7 NOV 2016
Accepted 13 DEC 2016
Accepted article online 15 DEC 2016
Published online 5 JAN 2017
Corrected 30 MAR 2017

This article was corrected on 30 MAR 2017. See the end of the full text for details.

Earthquake ground motion amplification for surface waves

Daniel C. Bowden[1] and **Victor C. Tsai**[1]

[1]Geological and Planetary Science Division, California Institute of Technology, Pasadena, California, USA

Abstract Surface waves from earthquakes are known to cause strong damage, especially for larger structures such as skyscrapers and bridges. However, common practice in characterizing seismic hazard at a specific site considers the effect of near-surface geology on only vertically propagating body waves. Here we show that surface waves have a unique and different frequency-dependent response to known geologic structure and that this amplification can be analytically calculated in a manner similar to current hazard practices. Applying this framework to amplification in the Los Angeles Basin, we find that peak ground accelerations for certain large regional earthquakes are underpredicted if surface waves are not properly accounted for and that the frequency of strongest ground motion amplification can be significantly different. Including surface-wave amplification in hazards calculations is therefore essential for accurate predictions of strong ground motion for future San Andreas Fault ruptures.

1. Introduction

A significant portion of the variability in earthquake ground motions is caused by local geological conditions immediately beneath a given site. It is well known, for example, that shallow sediments or soils can give rise to amplification and resonances as seismic waves propagate near vertically up to the surface [e.g., *Borcherdt and Gibbs*, 1976], notably occurring when wavelengths are 4 times the depth of the near-surface low-velocity layer. For this reason, it has become standard practice in earthquake engineering to use the local one-dimensional (1-D) shallow velocity structure at a site (or a proxy for it) [e.g., *Wills et al.*, 2000; *Wald and Allen*, 2007] to calculate the amount of local amplification that results for each site, as compared to a reference "hard rock" site [e.g., *Dobry et al.*, 1976; *Kramer*, 1996; *Kawase*, 2003]. Even when the actual 1-D geologic profile is not known, this description of vertical resonances underlies the interpretation of numerous empirical and observational approaches (e.g., single-site horizontal-to-vertical spectral ratio to determine peak resonance). While it is acknowledged that this description of vertically-incident shear waves does not capture the full variability of 3-D wave propagation effects [e.g., *Olsen and Schuster*, 1995; *Field et al.*, 2000; *Graves et al.*, 2011], the 1-D site term defined this way supplies a simple, consistent framework that can be practically implemented by engineers, providing the foundation for earthquake building codes and classifications [e.g., *Abrahamson and Shedlock*, 1997; *Dobry et al.*, 2000].

Here we show that site characterization calculations can be improved by accounting for surface-wave amplification in addition to the standard amplification of vertically propagating shear waves. It has long been recognized that surface waves propagate and amplify differently due to crustal heterogeneities [e.g., *Drake*, 1980; *Bard and Bouchon*, 1980; *Sánchez-Sesma*, 1987; *Kawase and Aki*, 1989; *Joyner*, 2000]. However, their amplification has been often ignored in site-specific estimates, partly due to the assumption that this amplification is challenging to model (e.g., requiring full-wavefield simulations) and that surface waves are most significant at periods not important for ordinary buildings [e.g., *Joyner*, 2000]. Contrary to both of these expectations, we show that application of analytic theory developed originally for long-period surface waves can be readily applied to the shorter-period ground motions important for earthquake hazards. While fully estimating the expected shaking from future events remains a complex problem, the definition of a site amplification term can be extended to include surface waves separately from that of vertically-incident shear waves.

2. Analytic Description

From long-period, global-scale, or tectonic-scale seismology studies [i.e., *Tromp and Dahlen*, 1992], it is known that conservation of energy flux requires that the relative surface-wave amplitudes between two sites satisfy

$$\frac{A_n}{A_n{}^R} = \frac{u_n(0)}{u_n{}^R(0)} \left(\frac{U I_0}{U^R I_0{}^R} \right)^{-1/2} \quad (1)$$

where $u_n(0)$ is the displacement eigenfunction measured at the surface (depth = 0) corresponding to the type of wave measured by A_n (where $n = 1$, 2, or 3 for radial, vertical, and tangential component of motion, respectively), U is group velocity, I_0 is an integral over the eigenfunctions and density, and superscript R refers to measurements at a reference site. Specifically, the term $1/(UI_0)$ describes a wave action potential [*Tromp and Dahlen*, 1992] and also appears in the standard formulation of surface-wave Green's functions [e.g., *Aki and Richards*, 2002] and is simply applied here in a hazard context. The I_0 integrals referred to in equation (1) are usually used to describe the kinetic energy of surface waves, used in the Lagrangian formulation to determine group and phase velocities. These integrals are defined differently for Rayleigh and Love waves as

$$\text{Rayleigh}: \; I_0 = \int_0^\infty \rho(z) \left(u_1(z)^2 + u_2(z)^2 \right) dz \quad (2)$$

$$\text{Love}: \quad I_0 = \int_0^\infty \rho(z) u_3(z)^2 dz \quad (3)$$

where ρ is density and z is depth. We note that the Rayleigh-wave eigenfunctions are usually normalized such that the vertical component of motion, u_2, is one at the surface. In this case, the $u_n/u_n{}^R$ term in equation (1) is simply one for vertical amplification at the surface, and for horizontal amplification, u_1 is the horizontal-to-vertical (H/V) ratio. Love waves are usually similarly normalized such that the term, u_3, is one at the surface. While the literature originally defining these amplitude relations considered surface-wave-potential amplitudes [*Tromp and Dahlen*, 1992], we are interested in displacements, and so we describe displacement amplitudes by multiplying the potentials by the corresponding eigenfunction to specify the component of motion considered.

The expression $A_n/A_n{}^R$ in equation (1) defines a frequency-dependent transfer function by which observations of ground motion at a reference site can be transformed to any other site, each described by a 1-D profile. Although this relation has typically been applied to only very long period surface waves (e.g., greater than 24 s by *Lin et al*. [2012]), the same physics applies to high-frequency surface waves as long as the velocity structure varies smoothly enough laterally [*Tromp and Dahlen*, 1992]. This description of relative local site amplification does not and should not include terms for path effects; anything that might affect the amplitudes due to the path of a ray such as focusing, attenuation, lateral basin resonance [e.g., *Bard and Bouchon*, 1985], or a conversion of wave types at sharp boundaries [e.g., *Liu and Heaton*, 1984; *Field*, 1996] is not described here, nor is this formulation concerned with the excitation of surface waves. Although the original formulation deals with conservation of energy traveling along a particular ray, in a site response context it can be applied to represent the transfer function between any two 1-D profiles, with the result describing the additional local amplification that would result by replacing the reference structure by the given site structure at any point. This is analogous to how a 1-D velocity profile is often used to calculate the standard vertically incident shear wave transfer function for engineering applications. For both types of waves, the locally 1-D assumption is still a simplification of reality [*Thompson et al*., 2009] but results in a useful, first-order quantification of how much ground motions are affected by local geology.

It may also be noted that Rayleigh waves can alternately be described as a superposition of *P* and *SV* waves, and similarly, Love waves can be described as trapped *SH* waves propagating and reflecting at a critical incidence angle. However, the near-horizontal incidence angle will also strongly affect the amplification strength and frequency [*Haskell*, 1960]. While other authors have noted that resonant shear waves may not be perfectly vertical and thus show some polarization [e.g., *Boore*, 2006], there is still a significant difference between such cases and fully developed surface waves.

3. Simple Basin Example

Figure 1 shows a comparison of site response terms calculated for both vertically-incident shear waves and surface waves in a simple sedimentary basin of 500 m depth, compared to a reference homogeneous half-space. The site response term for vertically incident shear waves is semianalytically estimated using a Thomson-Haskell propagator matrix approach [*Haskell*, 1953], although for this simple example a straightforward analytic solution also exists (for which the peak resonant frequency is $V_{s1}/4H$). Surface-wave

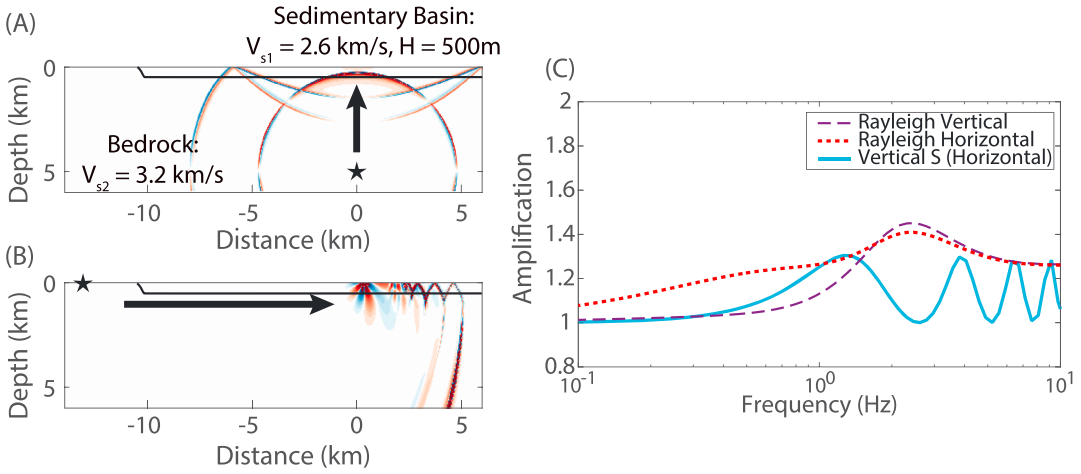

Figure 1. Comparison of amplification terms in a sedimentary basin, for (a) a vertically-incident shear wave or (b) a laterally propagating Rayleigh wave. The spectral amplification patterns (c) indicate that the two wave types interact with the low-velocity sedimentary layer in different ways. For this example, the shear wave velocity is set as 2.6 km/s in the basin and 3.2 km/s outside the basin. Note that for a more severe velocity contrast, all wave types would be more significantly amplified, but the comparison would be qualitatively similar.

eigenfunctions are also semianalytically estimated using Computer Programs in Seismology [*Herrmann*, 2013]. The medium for both wave types is purely elastic and without attenuation. Certainly, varying rates of attenuation and geometric spreading will play a significant role in the relative strengths of these wave types, but these are not part of the site amplification transfer function presented here.

Although both wave types are amplified, there is a significant quantitative difference for the surface waves entering this basin compared to the shear waves. For this idealized model, surface-wave amplification is roughly 50% stronger than and with a peak frequency twice that of the vertically-incident shear wave (see Figure 1c). Furthermore, although surface waves are often ignored at higher frequencies, it is these higher frequencies for which surface waves are most amplified. While other authors have observed the changing frequency content and amplitudes of surface-wave arrivals [e.g., *Pinnegar*, 2006], it is not generally considered that an entirely separate and unique transfer function can be used to describe the surface-wave system.

We note that the difference between the wave types' amplification spectra is persistent for other models. Even for a variety of tested basin depths, impedance contrasts and even for more realistic geologic profiles [e.g., *Boore and Joyner*, 1997], the differences in amplification remain (see supporting information Figure S1). Lastly, we note that these transfer functions are confirmed through 2-D finite difference simulations [*Li et al.*, 2014], with only minor differences caused by path effects such as scattering and a conversion of wave types at the edge of the sedimentary basin.

4. Application to a Southern California Velocity Model

This straightforward calculation of site terms can be implemented for any velocity model from which 1-D profiles can be extracted, including in Southern California, where recent developments of the Southern California Earthquake Center's Community Velocity Model (SCEC CVM-S4.26) [*Lee et al.*, 2014] facilitates this reexamination of seismic hazard. Efforts to account for surface waves are especially important for Southern California, where wavefronts from a future large earthquake on the San Andreas Fault system [*Graves et al.*, 2011] will enter the Los Angeles Basin laterally rather than from below (see Figure 1a). Figure 2 demonstrates the spatial variability of site terms at 0.4 Hz for each of a vertically-incident shear wave, Rayleigh wave (horizontal component), and Love wave, all relative to the hard rock site at station PASC in Pasadena and based only on 1-D profiles at each point. As expected, the depth of the Los Angeles sedimentary basin plays a significant role [e.g., *Hruby and Beresnev*, 2003; *Day et al.*, 2008]: the deepest region of the sedimentary basin causes surface waves to be strongly and consistently amplified, while vertically-incident shear waves do not all exhibit resonance given the variable basin shape. For

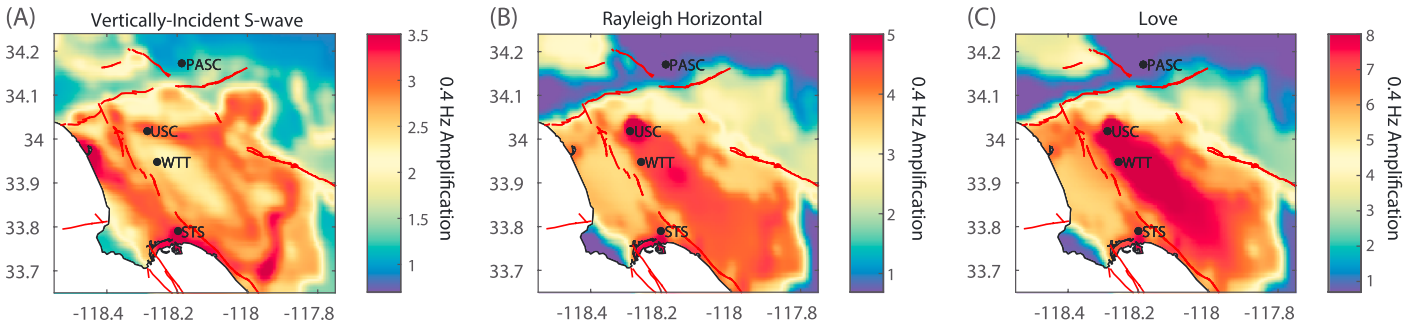

Figure 2. Maps of relative amplification for Southern California, describing 1-D amplification factors relative to the hard rock site, PASC, at 0.4 Hz for (a) vertically-incident shear waves, (b) horizontal component Rayleigh waves, and (c) Love waves. Faults from the *U.S. Geological Survey and California Geological Survey* [2006] are shown by red lines.

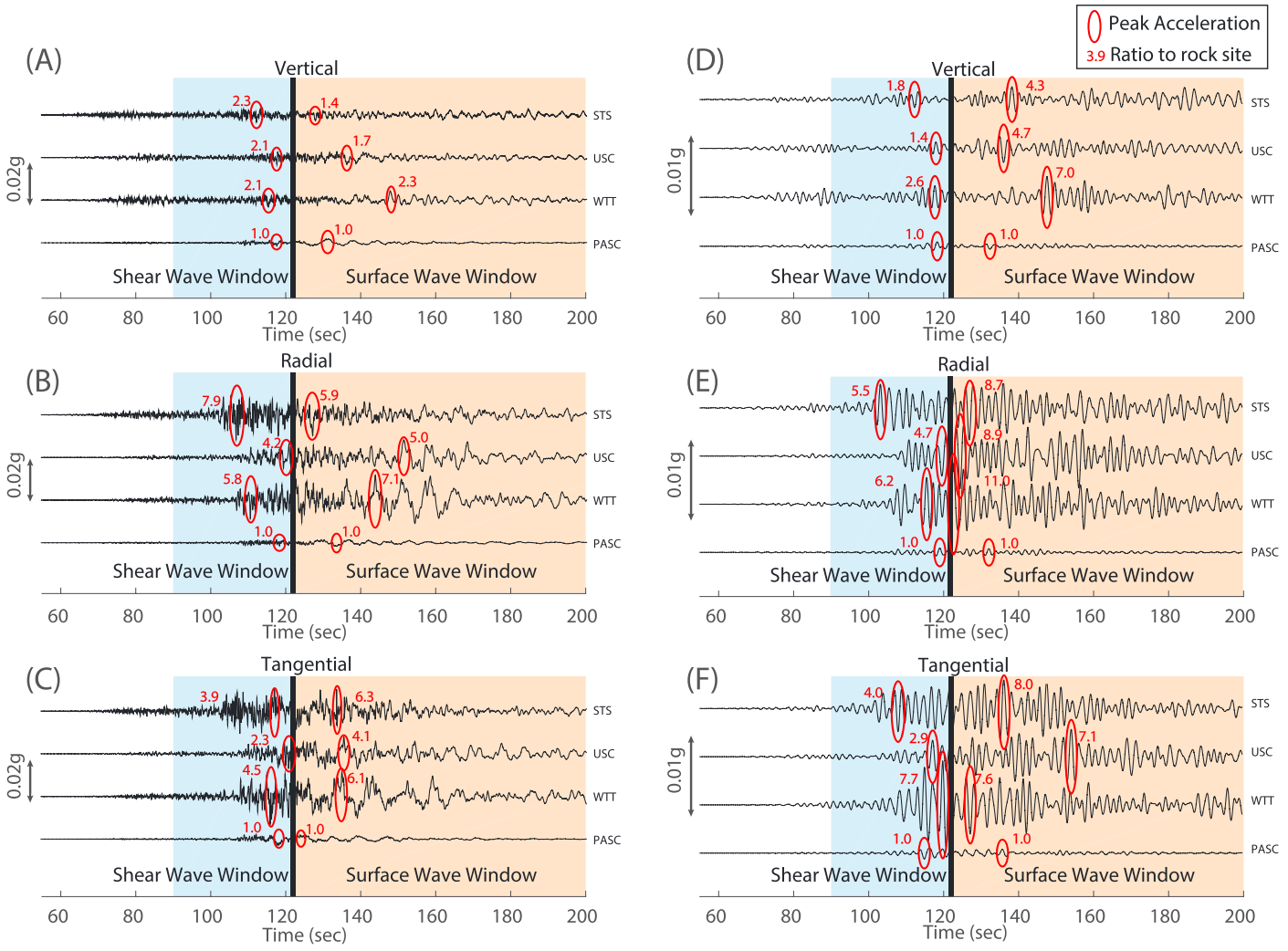

Figure 3. Acceleration waveforms comparing shear and surface waves, from the El Mayor Cucapah earthquake, *M*7.2, with its epicenter roughly 130 km to the SE of the Los Angeles Basin. (a–c) Unfiltered accelerations for vertical, radial, and tangential components, respectively. (d–f) Filtered at 0.3–0.7 Hz. In each panel, peak ground acceleration (PGA) is identified for shear waves and surface waves separately, and the ratio of this PGA to the hard rock site, PASC, is indicated.

example, the center of the basin near station WTT is too deep for resonance of vertically-incident shear wave at this period.

The Love-wave amplification predictions of Figure 2 are considerably higher than for the other wave types. This is partly because the geologic structure at our reference site, PASC, allows for little Love wave energy. On one hand, this may give a startling impression regarding the severity of Love waves in this basin, but it also serves to illustrate that if a hard rock reference station (like PASC) is used for any type of ground motion prediction or hazard estimate, Love waves will be significantly underpredicted from the analysis. The choice of a different reference bedrock site will affect the intensity of amplifications reported in these maps, though the dominant lateral features will remain.

Observations of ground motions confirm these differences in relative amplification. Specifically, we consider ground motions of the El Mayor Cucapah Earthquake, M_w7.2, which occurred SE of the Los Angeles Basin in 2010. Four stations are indicated in Figure 2, each a comparable distance and azimuth from the event such that attenuation and geometric spreading can be assumed comparable. Figures 3a–3c show the raw acceleration records, and we observe that the peak ground acceleration (PGA) relative to the hard rock site, PASC, is different when we consider shear wave arrivals separately from surface waves. While distinguishing surface waves from various body wave phases may often be difficult in practice (particularly for higher-frequency waves), we emphasize that PGA is often higher in the surface-wave window compared to the body-wave window (including for six of the nine basin ground motion records shown in Figure 3), despite the significant attenuation of high-frequency surface waves at this distance.

When comparing filtered waveforms (Figures 3d–3f), these differences are even more severe. At frequencies of 0.3–0.7 Hz, surface waves are amplified 2–3 times more strongly than shear waves, relative to the hard rock site, again commensurate with predictions from the SCEC CVM in Figure 2. Our division between shear-wave arrivals and surface-wave arrivals is based only on visual inspection of the hard rock site waveform, and some of the PGA peaks may be ambiguous or close to the boundary. As such, a more rigorous approach describing arrival energy with time could be applied or developed in the future [e.g., *Saikia et al*., 1994]. The predictions shown in Figure 2 do not account for path effects or other 3-D surface-wave phenomena, such as lateral basin resonance or conversion of wave types at sharp boundaries, yet the application of the appropriate 1-D site terms alone explains the most significant features of the waveforms, thus demonstrating the usefulness of the simplified 1-D amplification approach.

5. Discussion and Conclusions

In this work, we have shown that the nature of wave propagation results in different amounts of amplification by local geological structure for surface waves as compared to body waves. Moreover, a simple analytic theory can be applied to 1-D velocity structures to predict the amount of surface-wave amplification separately from the body wave amplification that is more commonly computed. The differences in site amplification spectra shown here indicate that if surface waves are to be included in any kind of hazard analysis, the analysis should include a frequency-dependent site response that is appropriate for surface waves. While some ground motion prediction equations include terms for the presence of basins or long-period signals [e.g., *Novikova and Trifunac*, 1994; *Campbell and Bozorgnia*, 2013], and therefore may implicitly account for surface-wave site response if the historical data contained these signals, application of the analytic theory used and described in this paper can explicitly account for surface waves independently of body waves and thus allow for the design of a more flexible and complete hazards model. Differences in source and path effects such as attenuation [e.g., *Mitchell*, 1973] and geometric spreading would also need to be accounted for, and this complexity suggests the importance of either simulations [e.g., *Graves et al*., 2010] or empirical observations [e.g., *Denolle et al*., 2014], which describe the full waveform. Nonetheless, describing a site-amplification term appropriate to each wave type represents a first step toward such an improved hazards model.

Independent of these considerations above, the differences in amplification spectra have implications for a broad range of hazard estimation techniques and the resulting interpretation. For example, if spectral ratios between two sites are measured, the existence of surface wave signals will fundamentally change the measurement [e.g., *Field*, 1996]. Conversely, if empirical records from a hard rock site are modified for use in structural response simulations at a sedimentary basin site, the later arrivals in the waveforms may be significantly misrepresented if only the standard, vertically-incident shear wave site term is applied. Cases where surface

waves ultimately contribute to the highest levels of ground motion may explain some of the epistemic variability observed in strong motion catalogs, since correlations with local geology or other proxies do not have the same relationship between surface waves and body waves. For all of these reasons, scientists and engineers need to be aware that a single definition of "site amplification" may be insufficient to describe both surface waves and body waves, in regard to both frequency and amplitude.

Acknowledgments
The velocity model used for Southern California is the SCEC CVM-S4.26, accessed from https://scec.usc.edu/scecpedia, on 25 February 2016, as part of the Unified Community Velocity Model package version 15.10.0. Seismograms are provided by the Caltech/USGS Southern California Seismic Network at http://scedc.caltech.edu. Surface-wave eigenfunctions are generated through R. Herrmann's Computer Programs in Seismology (available at http://www.eas.slu.edu/eqc/eqccps.html). Vertical transfer functions were validated against C. Mueller's NRATTLE script, provided as part of the SMSIM package by D. Boore (available at http://pubs.er.usgs.gov/publication/ofr00509). The authors thank Jian Shi, Fan-Chi Lin, Rob Clayton, and Raul Castro for their helpful discussion. We also thank Francisco Sánchez-Sesma and one anonymous reviewer for their helpful feedback in preparation of the manuscript. This work was supported by EAR-1252191, EAR-1453263, and SCEC-15035.

References

Abrahamson, N. A., and K. M. Shedlock (1997), Overview, *Seismol. Res. Lett.*, *68*(1), 9–23.
Aki, K., and P. G. Richards (2002), *Quantitative Seismology*, University Science Books, Sausalito, Calif.
Bard, P.-Y., and M. Bouchon (1980), The seismic response of sediment-filled valleys: Part 2. The case of incident *P* and *SV* waves, *Bull. Seismol. Soc. Am.*, *70*(5), 1921–1941.
Bard, P.-Y., and M. Bouchon (1985), The two-dimensional resonance of sediment-filled valleys, *Bull. Seismol. Soc. Am.*, *75*(2), 519–541.
Boore, D. M. (2006), Orientation-independent measures of ground motion, *Bull. Seismol. Soc. Am.*, *96*(4A), 1502–1511, doi:10.1785/0120050209.
Boore, D. M., and W. B. Joyner (1997), Site amplifications for generic rock sites, *Bull. Seismol. Soc. Am.*, *87*(2), 327–341.
Borcherdt, R. D., and J. F. Gibbs (1976), Effects of local geological conditions in the San Francisco Bay region on ground motions and the intensities of the 1906 earthquake, *Bull. Seismol. Soc. Am.*, *66*(2), 467–500.
Campbell, K. W., and Y. Bozorgnia (2013), NGA-West2 Campbell-Bozorgnia ground motion model for the horizontal components of PGA, PGV, and 5% damped elastic pseudo-acceleration response spectra for periods ranging from 0.01 to 10 sec, PEER Report 2013/06.
Day, S. M., R. Graves, J. Bielak, D. Dreger, S. Larsen, K. B. Olsen, A. Pitarka, and L. Ramirez-Guzman (2008), Model for basin effects on long-period response spectra in southern California, *Earthq. Spectra*, *24*(1), 257–277, doi:10.1193/1.2857545.
Denolle, M. A., H. Miyake, S. Nakagawa, N. Hirata, and G. C. Beroza (2014), Long-period seismic amplification in the Kanto Basin from the ambient seismic field, *Geophys. Res. Lett.*, *41*, 2319–2325, doi:10.1002/2014GL059425.
Dobry, R., I. Oweis, and A. Urzua (1976), Simplified procedures for estimating the fundamental period of a soil profile, *Bull. Seismol. Soc. Am.*, *66*(4), 1293–1321.
Dobry, R., R. D. Borcherdt, C. B. Crouse, I. M. Idriss, W. B. Joyner, G. R. Martin, M. S. Power, E. E. Rinne, and R. B. Seed (2000), New site coefficients and site classification system used in recent building code provisions, *Earthq. Spectra*, *16*(1), 41–67.
Drake, L. A. (1980), Love and Rayleigh waves in an irregular soil layer, *Bull. Seismol. Soc. Am.*, *70*(2), 571–582.
Field, E. H. (1996), Spectral amplification in a sediment-filled valley exhibiting clear basin-edge-induced waves, *Bull. Seismol. Soc. Am.*, *86*(4), 991–1005, doi:10.1130/0091-7613(2000)28<315:MWEFFA>2.0.CO;2.
Field, E. H., et al. (2000), Accounting for site effects in probabilistic seismic hazard analyses of southern California: Overview of the SCEC Phase III report, *Bull. Seismol. Soc. Am.*, *90*(6B), S1–S31, doi:10.1785/0120000512.
Graves, R. W., B. T. Aagaard, and K. W. Hudnut (2011), The ShakeOut earthquake source and ground motion simulations, *Earthq. Spectra*, *27*(2), 273–291, doi:10.1193/1.3570677.
Graves, R., et al. (2010), CyberShake: A physics-based seismic hazard model for Southern California, *Pure Appl. Geophys.*, *168*(3–4), 367–381, doi:10.1007/s00024-010-0161-6.
Haskell, N. A. (1953), The dispersion of surface waves on multilayered media, *Bull. Seismol. Soc. Am.*, *43*(1), 17–34.
Haskell, N. A. (1960), Crustal reflection of plane *SH* waves, *J. Geophys. Res.*, *65*, 4147–4150, doi:10.1029/JZ065i012p04147.
Herrmann, R. B. (2013), Computer programs in seismology: An evolving tool for instruction and research, *Seismol. Res. Lett.*, *84*(6), 1081–1088, doi:10.1785/0220110096.
Hruby, C. E., and I. A. Beresnev (2003), Empirical corrections for basin effects in stochastic ground-motion prediction, based on the Los Angeles basin analysis, *Bull. Seismol. Soc. Am.*, *93*(4), 1679–1690, doi:10.1785/0120020121.
Joyner, W. B. (2000), Strong motion from surface waves in deep sedimentary basins, *Bull. Seismol. Soc. Am.*, *90*(6), SUPPL. 95–112, doi:10.1785/0120000505.
Kawase, H. (2003), Site effects on strong ground motions, *Int. Handb. Earthquake Eng. Seismol.*, *81*, 1013.
Kawase, H., and K. Aki (1989), A study on the response of a soft basin for incident *S*, *P*, and Rayleigh waves with special reference to the long duration observed in Mexico City, *Bull. Seismol. Soc. Am.*, *79*(5), 1361–1382.
Kramer, S. L. (1996), *Geotechnical Earthquake Engineering*, Pearson Education, India.
Lee, E., P. Chen, T. H. Jordan, P. B. Maechling, M. A. M. Denolle, and G. C. Beroza (2014), Full-3-D tomography for crustal structure in Southern California based on the scattering-integral and the adjoint-wavefield methods, *J. Geophys. Res. Solid Earth*, *119*, 6421–6451, doi:10.1002/2014JB011346.
Li, D., D. Helmberger, R. W. Clayton, and D. Sun (2014), Global synthetic seismograms using a 2-D finite-difference method, *Geophys. J. Int.*, *197*(2), 1166–1183, doi:10.1093/gji/ggu050.
Lin, F.-C., V. C. Tsai, and M. H. Ritzwoller (2012), The local amplification of surface waves: A new observable to constrain elastic velocities, density, and anelastic attenuation, *J. Geophys. Res.*, *117*, B06302, doi:10.1029/2012JB009208.
Liu, H.-L., and T. Heaton (1984), Array analysis of the ground velocities and accelerations from the 1971 San Fernando, California, earthquake, *Bull. Seismol. Soc. Am.*, *74*(5), 1951–1968.
Mitchell, B. J. (1973), Surface-wave attenuation and crustal anelasticity in central North America, *Bull. Seismol. Soc. Am.*, *63*(3), 1057–1071.
Novikova, E. I., and M. D. Trifunac (1994), Duration of strong ground motion in terms of earthquake magnitude, epicentral distance, site conditions and site geometry, *Earthq. Eng. Struct. Dyn.*, *23*(November 1993), 1023–1043.
Olsen, K. B., and G. T. Schuster (1995), Causes of low-frequency ground motion amplification in the Salt Lake Basin: The case of the vertically incident *P* wave, *Geophys. J. Int.*, *122*(3), 1045–1061, doi:10.1111/j.1365-246X.1995.tb06854.x.
Pinnegar, C. R. (2006), Polarization analysis and polarization filtering of three-component signals with the time-frequency *S* transform, *Geophys. J. Int.*, *165*, 596–606, doi:10.1111/j.1365-246X.2006.02937.x.
Saikia, C. K., D. S. Dreger, and D. V. Helmberger (1994), Modeling of energy amplification recorded within Greater Los Angeles using irregular structure, *Bull. Seismol. Soc. Am.*, *84*(1), 47–61.
Sánchez-Sesma, F. J. (1987), Site effects on strong ground motion, *Soil Dyn. Earthq. Eng.*, *6*(2), 124–132.
Thompson, E. M., L. G. Baise, R. E. Kayen, and B. B. Guzina (2009), Impediments to predicting site response: Seismic property estimation and modeling simplifications, *Bull. Seismol. Soc. Am.*, *99*(5), 2927–2949, doi:10.1785/0120080224.

Tromp, J., and F. A. Dahlen (1992), Variational principles for surface wave propagation on a laterally heterogeneous Earth—II. Frequency-domain JWKB theory, *Geophys. J. Int.*, *109*, 599–619.

U.S. Geological Survey and California Geological Survey (2006), Quaternary fault and fold database for the United States, from USGS web site. [Available at http//earthquakes.usgs.gov/regional/qfaults/.]

Wald, D. J., and T. I. Allen (2007), Topographic slope as a proxy for seismic site conditions and amplification, *Bull. Seismol. Soc. Am.*, *97*(5), 1379–1395, doi:10.1785/0120060267.

Wills, C. J., M. Petersen, W. A. Bryant, M. Reichle, G. J. Saucedo, S. Tan, G. Taylor, and J. Treiman (2000), A site-conditions map for California based on geology and shear-wave velocity, *Bull. Seismol. Soc. Am.*, *90*(6B), S187–S208.

Erratum

In the originally published version of this article, Equation (1) incorrectly included terms for phase velocity, c or c^R, which were removed. Equations (2) and (3) incorrectly included a factor of z^2, which was removed.

In the paragraph following Eq. 1, the phrase "c is phase velocity" is removed.

In the sentence "Specifically, the term $1/(cUI_0)$ describes…" the c was removed.

Figures 1 and 2 have been updated to reflect the changes in Eq. 1.

The removal of the phase velocity term in Eq. 1 produced a small change; the amplification of horizontal and vertical Rayleigh waves were slightly reduced, and colorscale adjusted, but the shape and peak frequency remain the same. As such, the qualitative results, interpretation and conclusion remain unchanged. The z^2 in Eq. 2 and 3 was purely a typo – computations did not use this and do not need to be adjusted.

Text following Figure 1 is adjusted slightly. The sentence reading "For this idealized model, surface-wave amplification is roughly twice as strong and with a peak frequency twice that for the vertically-incident shear wave" should now read "For this idealized model, surface-wave amplification is roughly 50% stronger than and with a peak frequency twice that of the vertically-incident shear wave."

Finally, Figure S1 is updated as well. Again, the amplification curves for vertical Rayleigh, horizontal Rayleigh and Love waves are slightly reduced but the qualitative features and conclusions remain unchanged.

This version may be considered the authoritative version of record.